Imaging and Analysis of Single Optically Trapped Gold Nanoparticles Using Spatial Modulation Spectroscopy

ARTICLE *in* JOURNAL OF PHYSICAL CHEMISTRY LETTERS · AUGUST 2014

Impact Factor: 7.46 · DOI: 10.1021/jz501409q

3 AUTHORS:

Mary Sajini Devadas
Towson University
17 PUBLICATIONS **221** CITATIONS
SEE PROFILE

Zhongming Li
University of Notre Dame
5 PUBLICATIONS **13** CITATIONS
SEE PROFILE

Gregory V Hartland
University of Notre Dame
148 PUBLICATIONS **6,275** CITATIONS
SEE PROFILE

THE JOURNAL OF PHYSICAL CHEMISTRY Letters

Letter

pubs.acs.org/JPCL

Imaging and Analysis of Single Optically Trapped Gold Nanoparticles Using Spatial Modulation Spectroscopy

Mary Sajini Devadas,[†] Zhongming Li,[†] and Gregory V. Hartland*

Department of Chemistry and Biochemistry, University of Notre Dame, 251 Nieuwland Science Hall, Notre Dame, Indiana 46556-5670, United States

Supporting Information

ABSTRACT: The extinction cross sections and spectra of single nanoparticles can be directly measured by moving the particle in and out of a tightly focused laser beam. This technique, known as spatial modulation spectroscopy, yields detailed information about the size, shape, and environment of the particles. These experiments are typically done on particles immobilized on a substrate. Here we demonstrate for the first time the use of spatial modulation spectroscopy to interrogate single, optically trapped nanoparticles in solution. Gold nanoparticles as small as 15 nm were trapped and imaged. The experiments were performed by modulating the position of the probe laser beam while scanning it over the trapped particle with a galvo-scanning mirror system. This technique opens up the possibility of precisely measuring the optical properties of single nanoparticles in liquid environments, free from the influence of a surface.

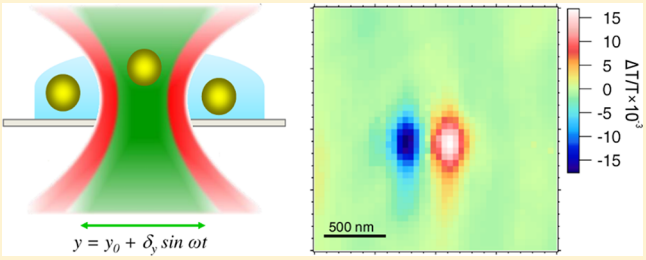

SECTION: Plasmonics, Optical Materials, and Hard Matter

Optical studies of nanoparticles is a major area of research, with applications to ultrasensitive detection as well as catalysis.[1−3] In conventional ensemble experiments, averaging over the different sizes present in the sample makes it difficult to precisely measure properties. This has made single-particle measurements an important tool for understanding how properties depend on the size, shape, and environment of the particles.[4,5] Single-particle measurements can be performed through absorption, scattering, or fluorescence detection. Although sensitive, fluorescence detection is not always possible, especially for metal nanoparticles, which are typically not strongly emissive.[6−8] Scattering methods are favorable for large nanoparticles (>20 nm diameter)[9] but fail at small sizes.[10] This has led to the development of absorption-based methods for interrogating single nanoparticles; examples include photothermal heterodyne imaging (PHI),[11−13] polarization modulation spectroscopy,[14,15] and spatial modulation spectroscopy (SMS).[16−26]

Of these different techniques, SMS is particularly useful because it allows the measurement of the absolute extinction cross-section of the nanoparticles, which is related to the volume of the particle.[16,27] SMS can be implemented by either moving the sample in-and-out of the laser focal spot[16−26] or by spatially modulating the beam at the sample.[28−30] These measurements are typically done for particles immobilized on a substrate. This creates an inhomogeneous environment that is difficult to accurately model by electromagnetic simulations and thus makes it hard to relate the measurements to the properties of the particles.[31,32] In this manuscript, SMS implemented with beam modulation is combined with optical trapping to interrogate single gold nanoparticles in solution, that is, in a completely homogeneous environment. Metal particles in optical traps have been analyzed in the past using light scattering[33−36] as well as transient absorption spectroscopy.[37] SMS is complementary to these techniques and offers advantages for full optical characterization of the size and shape of the particle.[27]

Figure 1 shows the layout of the optical setup. A single-beam 3D optical trap was created by tightly focusing a (nonresonant) near-IR laser beam into a dilute solution of the nanoparticles with a high numerical aperture (NA) objective.[33,38−40] For the larger particles studied, the power of the trapping beam was set to 60 mW at the sample (measured after transmission through the glass coverslip). For smaller particles, the power of the trap beam was increased to 140 mW. Single particles diffuse into the laser focus, where they can be stably trapped for tens of minutes. A probe laser beam (532 nm) was scanned over the particle using a galvo-scanning mirror (GSM) system. One of the mirrors in the GSM system was wobbled at 1 kHz, and a lock-in amplifier was used to measure the change in the transmitted power. This directly yields the extinction of the trapped gold particle.[16,17] A lock-in time constant of 10 ms and a 30 ms pixel dwell time were used in the experiments. The trapped particles were also imaged by a CMOS camera, which was used to determine when a particle had entered the trap.

Received: July 7, 2014
Accepted: August 11, 2014
Published: August 11, 2014

   dx.doi.org/10.1021/jz501409q | J. Phys. Chem. Lett. 2014, 5, 2910−2915

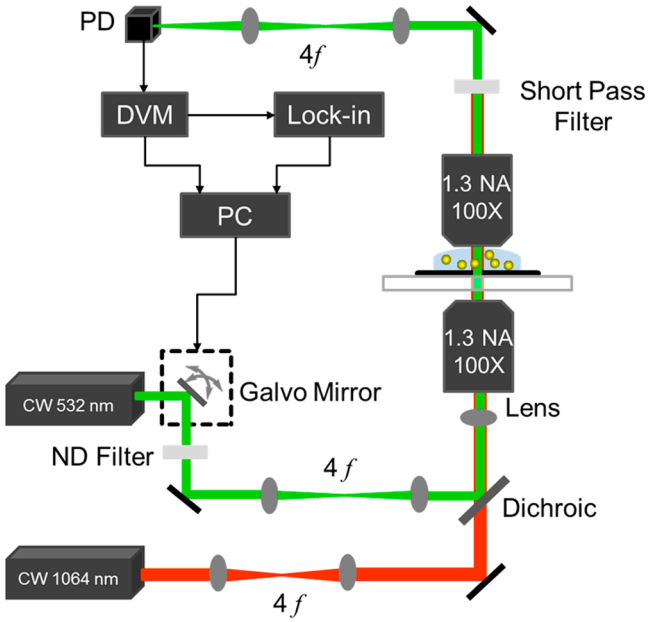

Figure 1. Schematic of the experimental setup for SMS measurements of optically trapped gold nanoparticles using galvo-scanning mirrors. DVM, digital voltmeter; ND, neutral density filter; PD, photodiode; 4*f*, 4*f* lens system.

For a nanoparticle at the focus of a high NA objective, the transmitted power P_t of the laser beam is given by $P_t = P_i - \sigma_{ext} I(x, y)$, where P_i is the incident power, $I(x,y)$ is the intensity of the beam at the position of the particle, and σ_{ext} is the extinction cross-section.[16,17] For a small modulation of either the particle or beam position, the transmitted power can be Taylor-expanded into a Fourier series for the modulation frequency. The coefficients for the different frequency terms involve σ_{ext}, the spot size of the laser beam (w_0), the degree of modulation δ, and the first, second, third, and so on derivatives of $I(x,y)$.[16,17] These different terms can be separately measured by a lock-in amplifier. The majority of the experiments in this paper were performed at the first harmonic of the lock-in amplifier. In this case, for modulation in the x direction and assuming a Gaussian profile for the laser beam, the signal is given by

$$\frac{\Delta P}{P} = \frac{8}{\pi} \cdot \frac{\sigma_{ext}\delta}{w_0^4} \cdot x \cdot e^{-2(x^2+y^2)/w_0^2} \quad (1)$$

Fitting the data thus yields the extinction cross-section σ_{ext} and spot size w_0 given that δ is known. Note that eq 1 will not give accurate values for σ_{ext} if the beam strongly deviates from a Gaussian profile.

Figure 2A–D shows SMS images (4 μm × 4 μm) obtained for a large (~50 nm) gold nanoparticle trapped in water. Figure 2A is a contour plot recorded at the fundamental frequency *f*, and Figure 2C is an image recorded at the second-harmonic 2*f*. These images are typical of SMS experiments on immobilized nanoparticles.[16,17] Figure 2B,D shows line profiles from the images, along with a fit to the data. The fitting parameters were the beam diameter and extinction cross-section. For this particle, σ_{ext} = 5630 ± 470 nm^2 and w_0 = 620 ± 10 nm. This cross-section corresponds to a particle with a diameter of 47 ± 1 nm, and the signal-to-noise ratio for this experiment was 100:1. The spot size of the probe beam determined from the SMS data was consistent with the value of 640 ± 13 nm recorded by the CMOS camera. (See the Supporting Information.) The spot size of the trapping beam was also evaluated using the camera and was determined to be 930 ± 18 nm.

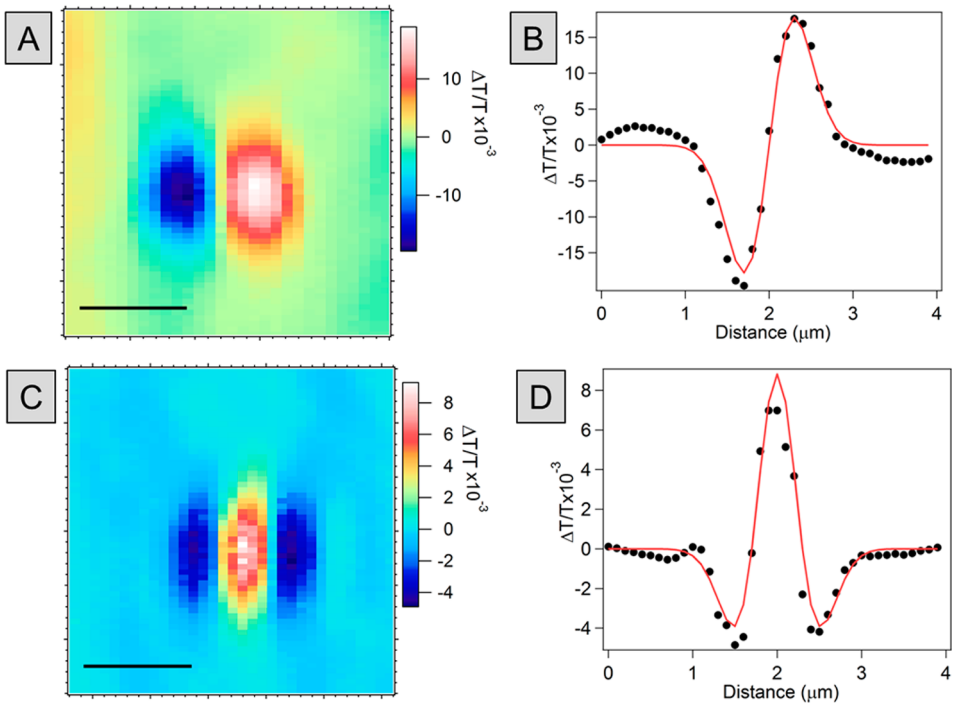

Figure 2. (A) 1*f* Contour plot of a 47 ± 1 nm trapped particle in water. (B) Line profile along with fit to the data. (C) 2*f* Contour plot of the same particle. (D) Line profile and fit of the particle in panel C. Data were recorded with a lock-in time constant of 10 ms and pixel dwell time of 30 ms. The power of the trapping laser (1064 nm) was 60 mW, and the power of the imaging laser (532 nm) was 60 μW. Scale bars are 1 μm.

dx.doi.org/10.1021/jz501409q | J. Phys. Chem. Lett. 2014, 5, 2910–2915

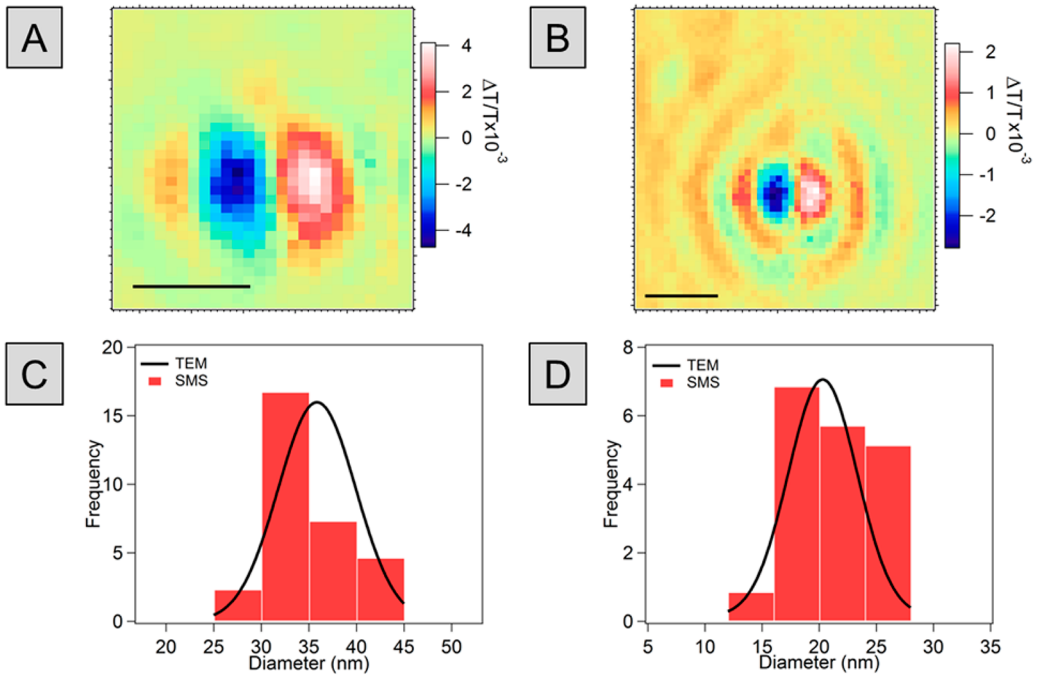

Figure 3. (A) 1*f* Contour plot of a particle from the 36 ± 5 nm sample and (B) 1*f* contour plot of a particle from the 19 ± 4 nm sample. Data were recorded with a lock-in time constant of 10 ms and pixel dwell time of 30 ms. Power of the trapping laser was 60 mW for panel A and 140 mW for panel B. Scale bars are 1 μm. Panels C and D show histograms of the diameter of the particles calculated from the SMS experiments. The solid lines are the size distributions determined from the TEM image analysis.

Detailed SMS experiments were conducted on two samples with average diameters of 36 ± 5 nm (NP1) and 19 ± 4 nm (NP2) to determine the sensitivity and accuracy of the technique. (The size distributions were measured using TEM; see the Supporting Information.) Figure 3A,B shows representative SMS images of trapped particles from the NP1 and NP2 samples, respectively, recorded at the fundamental frequency *f*. The corresponding fits (not shown) give σ_{ext} = 1010 ± 60 nm^2 for the particle in Figure 3A, and σ_{ext} = 580 ± 30 nm^2 for the particle in Figure 3B. For Figure 3A, the signal-to-noise ratio was 40:1 compared with 20:1 for Figure 3B. Figure 3C shows a histogram of the diameters of the trapped particles from NP1 determined by SMS. 44 particles were analyzed, and the cross sections were converted to diameter by comparison with Mie theory calculations.[5] The line shows the expected size distribution determined from the TEM measurements. The average diameter measured by the SMS experiments was 31 ± 5 nm for NP1, in good agreement with the TEM analysis. Similarly, Figure 3D shows a histogram of the diameters measured by SMS for NP2 (39 particles analyzed). The average size determined from the SMS measurements was 18 ± 7 nm, again in good agreement with the TEM analysis. Note that a higher power was used for the trapping laser for the smaller particles (140 mW for NP2 compared with 60 mW for NP1). The good agreement between the size distributions measured by SMS and TEM for the two samples demonstrates the accuracy of the SMS measurements and indicates that aberrations in the beam, which are clearly present in the image presented in Figure 3B, do not significantly affect the derived cross sections.

Another issue that is important to examine in these experiments is the effect of the trapping laser on the measured cross sections. Heating from the trap beam could broaden the plasmon resonance of the particle and thus change the extinction cross-section.[41] Figure 4A shows results for the same particle with the trapping laser turned on and off. These experiments were performed on an immobilized ~30 nm gold particle on a glass coverslip, with water added to the sample. The inserts show the contour plots of the data. The cross sections obtained by fitting the data in Figure 4A are 1026 ± 50 and 1030 ± 57 nm^2 for the particle with and without the trapping laser, respectively. In these fits, the beam size was held fixed at a value 600 nm. These results show that there is essentially no change in the cross-section with the trapping laser present, which implies that heating by the trap beam does not affect the measurement at the powers used in these experiments.

The data in Figure 3 show that we are able to detect particles as small as 15 nm diameter with reasonable signal-to-noise. In general, the signal-to-noise in these experiments is worse than that for SMS measurements performed on particles immobilized on a substrate by roughly a factor of 2. We believe that this is due to two effects. First, it is hard to exactly focus the probe beam onto the trapped particle. Slight differences in the focal plane of the probe compared with the trapping plane will degrade the signal. Second, the particles are not perfectly still in the trap, and small motions can cause noise in the SMS measurements. Figure 4B shows a time trace for a trapped particle that demonstrates that the dominant source of noise in the signal arises from the particle. In this experiment, the magnitude of the signal ($R = (X^2 + Y^2)^{1/2}$) was measured at the fundamental (1*f*) frequency, with a time constant of 10 ms and a 30 ms integration time. At ca. 400 s, the near-IR beam was blocked to release the particle from the trap. The noise is clearly worse when the particle is trapped, indicating that the noise does not arise from the laser or the detection system but is due to the presence of the particle in the trap.

dx.doi.org/10.1021/jz501409q | *J. Phys. Chem. Lett.* 2014, 5, 2910−2915

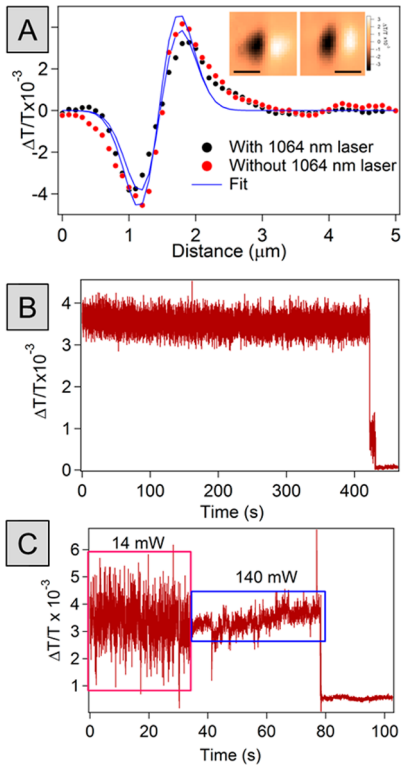

Figure 4. (A) Line profile comparisons for a 30 nm particle spin-coated on a coverslip to determine the effect of the trapping laser on the cross-section. Inserts are images of the same particle with only the probe (left) and with probe beam and the trapping beam (right). Scale bars =1 μm in all figures. (B) Time trace of a trapped nanoparticle obtained by overlapping the probe and trap beams for a 19 nm particle. The drop in signal at 400 s is due to blocking the trapping laser. The power of the trapping laser was set to 60 mW at the sample for panels A and B. (C) Time trace of a 39 nm particle demonstrating the change in the noise level of the SMS signal with increased trap stiffness. The time constant was 10 ms and integration time was 30 ms.

This source of noise could be improved by improving the trap stiffness (for example, by using a higher NA objective or by increasing the trapping power) or by performing the measurements at higher frequency.[37] Currently, it is not possible to significantly increase the frequency of the SMS measurement, and thus we focus on the trap stiffness. Figure 4C shows an experiment where the magnitude of the SMS signal is recorded for a trapped particle at a low laser power, and the power is then increased while the particle is trapped. The noise clearly decreases at higher trap power, showing that the dominant noise source in these experiments arises from the motion of the particle in the trap. Note that it is not possible to arbitrarily increase the trapping laser power to create very stiff traps in our system, as this leads to multiple particles being held in the trap. An SMS image where two particles are present in the trap is presented in the Supporting Information. The particles in this case were quite large (from a different sample than those in Figures 2−4), and are clearly well-separated in the image. This image demonstrates the possibility of using these experiments to interrogate the properties of complex plasmonic structures in solution.

The stiffness of the trap in our experiments was measured by the drag force method. (See the Supporting Information for details.)[42,43] For ca. 40 nm gold particles, these measurements give a trap stiffness of 0.00066 ± 0.00005 pN/nm for a trapping power of 100 mW. This value is in reasonable agreement with results from other groups; see, for example, ref 39. Interestingly, we note that the trap stiffness decreases when the probe laser is present. For a typical probe power of 420 μW, the stiffness is reduced to 0.00015 ± 0.00003 pN/nm. The reduction in trap stiffness when the probe is present could be due to heating by the probe, which could reduce the viscosity of the liquid around the particle and therefore allow greater freedom for random motion for the particle.[44,45] Another possibility is that radiation pressure from the probe laser could push the particle out of the trap.[40] Note that these effects could be reduced by decreasing the probe laser power. However, this will also reduce the signal-to-noise in the experiments due to poorer photon counting statistics. Optimizing these experiments to achieve signal-to-noise ratios comparable to what can be done for substrate supported particles is clearly a challenge.

In conclusion, we have shown that SMS can be used to interrogate optically trapped nanoparticles as small as 15 nm. This technique offers several advantages over conventional light-scattering-based methods to analyze trapped nanoparticles: First, in principle, smaller nanoparticles can be examined by absorption-based techniques compared with light scattering.[10] Second, SMS gives absolute values of the extinction cross-section, which is useful for determining the size of the trapped nano-object.[16,17] The extension of these experiments to record spectra, like what has been done for substrate supported particles,[27] should be straightforward and will be extremely useful for studying the spectroscopy of metal nanostructures. In particular, optically trapped particles experience a homogeneous environment, which can be much more accurately modeled compared with substrate supported particles. This will allow more precise comparison between experiment and theory.

■ EXPERIMENTAL METHODS

The linearly polarized output from a 1064 nm Ytterbium fiber laser (iPG Photonics Corporation 6W, YLR -5-1064-LP) was used as the trapping laser. The laser was focused down to a diffraction-limited spot using a high NA objective (Olympus UPlan FLN, 100× 1.3 NA). To correct for spherical aberrations due to the fluid (water), we placed a 50 cm lens in the beam path just before the objective.[37,46] The size of the trapping beam was adjusted to overfill the back-aperture of the objective. The probe beam was obtained from a 532 nm CW laser (Spectra Physics, Millennia Vs). The probe was directed through a GSM system (Thorlabs, GVSM002) before being combined with the trapping laser by a dichroic mirror (Thorlabs, DMLP900). A second high-NA objective was used to recollimate the probe beam, and the trapping beam was eliminated using a short-pass filter (Thorlabs, FGB37). The GSM system was used to scan the probe over the trapped particle as well as to modulate the position of the probe at the sample. This was achieved by combining the control voltage generated from our data acquisition program with the reference output from a lock-in amplifier (Stanford Research Instruments, SR 830). The voltage of the reference was adjusted to give a 0.2 μm modulation at the sample. 4*f* lens systems were used to project the probe beam from the GSM system to the back aperture of the focusing objective, and from the back aperture of the collimation objective to the detector (Thorlabs PDA36A Si photodiode, PD).[28] The DC component of the PD signal was recorded with a digital voltmeter (Keithley, 2000 Multimeter), and the in-phase component of the modulated

dx.doi.org/10.1021/jz501409q | J. Phys. Chem. Lett. 2014, 5, 2910−2915

signal was recorded by the lock-in amplifier. The background in the SMS experiments was reduced by careful alignment through the lens systems to $\Delta I/I < 10^{-5}$ without the sample, which is similar to the background levels in SMS experiments implemented with a piezo-stage.[16,17] The microscope used for the experiments (Olympus IX71) was fitted with a CMOS camera (Thor Laboratories DCC1645C-HQ) to align the beams and to determine when a particle has entered the trap.

The nanoparticles used for these experiments were prepared by the standard wet chemical citrate reduction method, as described by Frens.[47] The samples were characterized using transmission electron microscopy (TEM, JEOL 2010) and UV−vis spectroscopy. (See the Supporting Information.) TEM images were obtained by drop-casting the as-prepared solutions onto a Formvar-coated Cu grid. The size distribution was calculated using ImageJ. The size distributions of the two samples used in the experiments were 36 ± 5 and 19 ± 4 nm respectively. (See the Supporting Information.) For all optical experiments a sufficiently dilute nanoparticle solution in water was used (1:4000 dilution factor) to prevent multiply trapped particles. About 100 μL of sample was placed on a coverslip, and experiments were done in an open-access configuration without a flow cell.

■ ASSOCIATED CONTENT

Supporting Information

Transmission electron microscopy images and UV−visible absorption spectra of the gold nanoparticles used in the experiments; optical characterization of the beam size at the microscope focus, additional details of the trap stiffness measurements, and the Mathematica script used to calculate the extinction cross sections of the particles. This material is available free of charge via the Internet at http://pubs.acs.org.

■ AUTHOR INFORMATION

Corresponding Author

*E-mail: ghartlan@nd.edu.

Author Contributions

†M.S.D. and Z.L. contributed equally.

Notes

The authors declare no competing financial interest.

■ ACKNOWLEDGMENTS

This work was supported by the National Science Foundation (CHE-1110560), the Office of Naval Research (Award No.: N00014-12-1-1030), and the University of Notre Dame Strategic Research Initiative.

■ REFERENCES

(1) Willets, K. A.; Van Duyne, R. P. Localized Surface Plasmon Resonance Spectroscopy and Sensing. *Annu. Rev. Phys. Chem.* **2007**, *58*, 267−297.

(2) Raschke, G.; Kowarik, S.; Franzl, T.; Sonnichsen, C.; Klar, T. A.; Feldmann, J.; Nichtl, A.; Kurzinger, K. Biomolecular Recognition Based on Single Gold Nanoparticle Light Scattering. *Nano Lett.* **2003**, *3*, 935−938.

(3) Xu, W. L.; Kong, J. S.; Yeh, Y. T. E.; Chen, P. Single-molecule Nanocatalysis Reveals Heterogeneous Reaction Pathways and Catalytic Dynamics. *Nat. Mater.* **2008**, *7*, 992−996.

(4) Slaughter, L.; Chang, W.-S.; Link, S. Characterizing Plasmons in Nanoparticles and Their Assemblies with Single Particle Spectroscopy. *J. Phys. Chem. Lett.* **2011**, *2*, 2015−2023.

(5) Hartland, G. V. Optical Studies of Dynamics in Noble Metal Nanostructures. *Chem. Rev.* **2011**, *111*, 3858−3887.

(6) Fang, Y.; Chang, W.-S.; Willingham, B.; Swanglap, P.; Dominguez-Medina, S.; Link, S. Plasmon Emission Quantum Yield of Single Gold Nanorods as a Function of Aspect Ratio. *ACS Nano* **2012**, *6*, 7177−7184.

(7) Tcherniak, A.; Dominguez-Medina, S.; Chang, W.-S.; Swanglap, P.; Slaughter, L. S.; Landes, C. F.; Link, S. One-Photon Plasmon Luminescence and Its Application to Correlation Spectroscopy as a Probe for Rotational and Translational Dynamics of Gold Nanorods. *J. Phys. Chem. C* **2011**, *115*, 15938−15949.

(8) Yorulmaz, M.; Khatua, S.; Zijlstra, P.; Gaiduk, A.; Orrit, M. Luminescence Quantum Yield of Single Gold Nanorods. *Nano Lett.* **2012**, *12*, 4385−4391.

(9) Sonnichsen, C.; Franzl, T.; Wilk, T.; von Plessen, G.; Feldmann, J. Plasmon Resonances in Large Noble-Metal Clusters. *New J. Phys.* **2002**, *4*, 93.91−93.98.

(10) van Dijk, M. A.; Tchebotareva, A. L.; Orrit, M.; Lippitz, M.; Berciaud, S.; Lasne, D.; Cognet, L.; Lounis, B. Absorption and Scattering Microscopy of Single Metal Nanoparticles. *Phys. Chem. Chem. Phys.* **2006**, *8*, 3486−3495.

(11) Boyer, D.; Tamarat, P.; Maali, A.; Lounis, B.; Orrit, M. Photothermal Imaging of Nanometer-Sized Metal Particles among Scatterers. *Science* **2002**, *297*, 1160−1163.

(12) Berciaud, S. P.; Cognet, L.; Blab, G. A.; Lounis, B. Photothermal Heterodyne Imaging of Individual Nonfluorescent Nanoclusters and Nanocrystals. *Phys. Rev. Lett.* **2004**, *93*, 257402.

(13) Berciaud, S. P.; Lasne, D.; Blab, G. A.; Cognet, L.; Lounis, B. Photothermal Heterodyne Imaging of Individual Ietallic Nanoparticles: Theory versus Experiment. *Phys. Rev. B* **2006**, *73*, 045424.

(14) Carey, C. R.; LeBel, T.; Crisostomo, D.; Giblin, J.; Kuno, M.; Hartland, G. V. Imaging and Absolute Extinction Cross-Section Measurements of Nanorods and Nanowires through Polarization Modulation Microscopy. *J. Phys. Chem. C* **2010**, *114*, 16029−16036.

(15) Lefebvre, J.; Finnie, P. Polarized Light Microscopy and Spectroscopy of Individual Single-Walled Carbon Nanotubes. *Nano Res.* **2011**, *4*, 788−794.

(16) Arbouet, A.; Christofilos, D.; Del Fatti, N.; Vallée, F.; Huntzinger, J. R.; Arnaud, L.; Billaud, P.; Broyer, M. Direct Measurement of the Single-Metal-Cluster Optical Absorption. *Phys. Rev. Lett.* **2004**, *93*, 127401.

(17) Billaud, P.; Marhaba, S.; Cottancin, E.; Arnaud, L.; Bachelier, G.; Bonnet, C.; Del Fatti, N.; Lerme, J.; Vallee, F.; Vialle, J. L.; et al. Correlation Between the Extinction Spectrum of a Single Metal Nanoparticle and Its Electron Microscopy Image. *J. Phys. Chem. C* **2008**, *112*, 978−982.

(18) Muskens, O. L.; Bachelier, G.; Del Fatti, N.; Vallee, F.; Brioude, A.; Jiang, X.; Pileni, M.-P. Quantitative Absorption Spectroscopy of a Single Gold Nanorod. *J. Phys. Chem. C* **2008**, *112*, 8917−8921.

(19) Muskens, O. L.; Billaud, P.; Broyer, M.; Del Fatti, N.; Vallee, F. Optical Extinction Spectrum of a Single Metal Nanoparticle: Quantitative Characterization of a Particle and of its Local Environment. *Phys. Rev. B* **2008**, *78*, 205410.

(20) Baida, H.; Billaud, P.; Marhaba, S.; Christofilos, D.; Cottancin, E.; Crut, A.; Lerme, J.; Maioli, P.; Pellarin, M.; Broyer, M.; et al. Quantitative Determination of the Size Dependence of Surface Plasmon Resonance Damping in Single Ag@SiO2 Nanoparticles. *Nano Lett.* **2009**, *9*, 3463−3469.

(21) Lerme, J.; Baida, H.; Bonnet, C.; Broyer, M.; Cottancin, E.; Crut, A.; Maioli, P.; Del Fatti, N.; Vallee, F.; Pellarin, M. Size Dependence of the Surface Plasmon Resonance Damping in Metal Nanospheres. *J. Phys. Chem. Lett.* **2010**, *1*, 2922−2928.

(22) Lombardi, A.; Loumaigne, M.; Crut, A.; Maioli, P.; Del Fatti, N.; Vallee, F.; Spuch-Calvar, M.; Burgin, J.; Majimel, J.; Treguer-Delapierre, M. Surface Plasmon Resonance Properties of Single Elongated Nanoobjects: Gold Nanobipyramids and Nanorods. *Langmuir* **2012**, *28*, 9027−9033.

(23) Juve, V.; Fernanda Cardinal, M.; Lombardi, A.; Crut, A.; Maioli, P.; Perez-Juste, J.; Liz-Marzan, L. M.; Del Fatti, N.; Vallee, F. Size-

Dependent Surface Plasmon Resonance Broadening in Nonspherical Nanoparticles: Single Gold Nanorods. *Nano Lett.* **2013**, *13*, 2234−2240.
(24) Lombardi, A.; Grzelczak, M. P.; Crut, A.; Maioli, P.; Pastoriza-Santos, I.; Liz-Marzan, L. M.; Del Fatti, N.; Vallee, F. Optical Response of Individual Au-Ag@SiO2 Heterodimers. *ACS Nano* **2013**, *7*, 2522−2531.
(25) Oudjedi, L.; Parra-Vasquez, A. N. G.; Godin, A. G.; Cognet, L.; Lounis, B. Metrological Investigation of the (6,5) Carbon Nanotube Absorption Cross Section. *J. Phys. Chem. Lett.* **2013**, *4*, 1460−1464.
(26) McDonald, M. P.; Vietmeyer, F.; Aleksiuk, D.; Kuno, M. Supercontinuum Spatial Modulation Spectroscopy: Detection and Noise Limitations. *Rev. Sci. Instrum.* **2013**, *84*, 113104.
(27) Crut, A.; Maioli, P.; Del Fatti, N.; Vallee, F. Optical Absorption and Scattering Spectroscopies of Single Nano-Objects. *Chem. Soc. Rev.* **2014**, *43*, 3921−3956.
(28) Devadas, M. S.; Li, Z.; Major, T. A.; Lo, S. S.; Havard, N.; Yu, K.; Johns, P.; Hartland, G. V. Detection of Single Sold Nanoparticles using Spatial Modulation Spectroscopy Implemented with a Galvo-Scanning Mirror System. *Appl. Opt.* **2013**, *52*, 7806−7811.
(29) Havard, N.; Li, Z.; Murthy, V.; Lo, S. S.; Hartland, G. V. Spatial Modulation Spectroscopy of Graphene Sheets. *J. Chem. Phys.* **2014**, *140*, 074203.
(30) Fairbairn, N.; Light, R. A.; Carter, R.; Fernandes, R.; Kanaras, A. G.; Elliott, T. J.; Somekh, M. G.; Pitter, M. C.; Muskens, O. L. Spatial Modulation Microscopy for Real-Time Imaging of Plasmonic Nanoparticles and Cells. *Opt. Lett.* **2012**, *37*, 3015−3017.
(31) Davletshin, Y. R.; Lombardi, A.; Fernanda Cardinal, M.; Juve, V.; Crut, A.; Maioli, P.; Liz-Marzan, L. M.; Vallee, F.; Del Fatti, N.; Kumaradas, J. C. A Quantitative Study of the Environmental Effects on the Optical Response of Gold Nanorods. *ACS Nano* **2012**, *6*, 8183−8193.
(32) Lerme, J.; Bonnet, C.; Broyer, M.; Cottancin, E.; Manchon, D.; Pellarin, M. Optical Properties of a Particle above a Dielectric Interface: Cross Sections, Benchmark Calculations, and Analysis of the Intrinsic Substrate Effects. *J. Phys. Chem. C* **2013**, *117*, 6383−6398.
(33) Bosanac, L.; Aabo, T.; Bendix, P. M.; Oddershede, L. B. Efficient Optical Trapping and Visualization of Silver Nanoparticles. *Nano Lett.* **2008**, *8*, 1486−1491.
(34) Guffey, M. J.; Scherer, N. F. All-Optical Patterning of Au Nanoparticles on Surfaces Using Optical Traps. *Nano Lett.* **2010**, *10*, 4302−4308.
(35) Ruijgrok, P. V.; Verhart, N. R.; Zijlstra, P.; Tchebotareva, A. L.; Orrit, M. Brownian Fluctuations and Heating of an Optically Aligned Gold Nanorod. *Phys. Rev. Lett.* **2011**, *107*, 037401.
(36) Ohlinger, A.; Nedev, S.; Lutich, A. A.; Feldmann, J. Optothermal Escape of Plasmonically Coupled Silver Nanoparticles from a Three-Dimensional Optical Trap. *Nano Lett.* **2011**, *11*, 1770−1774.
(37) Ruijgrok, P. V.; Zijlstra, P.; Tchebotareva, A. L.; Orrit, M. Damping of Acoustic Vibrations of Single Gold Nanoparticles Optically Trapped in Water. *Nano Lett.* **2012**, *12*, 1063−1069.
(38) Ashkin, A.; Dziedzic, J. M.; Bjorkholm, J. E.; Chu, S. Observation of a Single-Beam Gradient Force Optical Trap for Dielectric Particles. *Opt. Lett.* **1986**, *11*, 288−290.
(39) Hansen, P. M.; Bhatia, V. K. l.; Harrit, N.; Oddershede, L. Expanding the Optical Trapping Range of Gold Nanoparticles. *Nano Lett.* **2005**, *5*, 1937−1942.
(40) Richard, W. B.; Miles, J. P. Optical Trapping and Binding. *Rep. Prog. Phys.* **2013**, *76*, 026401.
(41) Hodak, J. H.; Martini, I.; Hartland, G. V. Spectroscopy and Dynamics of Nanometer-Sized Noble Metal Particles. *J. Phys. Chem. B* **1998**, *102*, 6958−6967.
(42) Neuman, K. C.; Block, S. M. Optical Trapping. *Rev. Sci. Instrum.* **2004**, *75*, 2787−2809.
(43) Malagnino, N.; Pesce, G.; Sasso, A.; Arimondo, E. Measurements of Trapping Efficiency and Stiffness in Optical Tweezers. *Opt. Commun.* **2002**, *214*, 15−24.
(44) Raduenz, R.; Rings, D.; Kroy, K.; Cichos, F. Hot Brownian Particles and Photothermal Correlation Spectroscopy. *J. Phys. Chem. A* **2009**, *113*, 1674−1677.
(45) Rings, D.; Schachoff, R.; Selmke, M.; Cichos, F.; Kroy, K. Hot Brownian Motion. *Phys. Rev. Lett.* **2010**, *105*, 090604.
(46) Hajizadeh, F.; Reihani, S. N. Optimized Optical Trapping of Gold Nanoparticles. *Opt. Express* **2010**, *18*, 551−559.
(47) Frens, G. Controlled Nucleation for Regulation of Particle-Size In Monodisperse Gold Suspensions. *Nat. Phys. Sci.* **1973**, *241*, 20−22.